Fabrication of Electrochemical Biosensor Using Zinc Oxide Nanoflowers for the Detection of Uric Acid

priyanka dutta
CSIR-NPL: National Physical Laboratory CSIR
Vikas sharma
CSIR-NPL: National Physical Laboratory CSIR
Hema bhardwaj
CSIR-NPL: National Physical Laboratory CSIR
ved varun agrawal
CSIR-NPL: National Physical Laboratory CSIR
Rajesh nil
CSIR-NPL: National Physical Laboratory CSIR
gajjala sumana (gajjalasumana19@gmail.com)
CSIR-NPL: National Physical Laboratory CSIR https://orcid.org/0000-0003-2948-8006

Research Article

Keywords: Uric acid, Uricase, Horseradish Peroxidase, ZnONFs, Cyclic Voltammetry, Urea.

Posted Date: July 29th, 2021

DOI: https://doi.org/10.21203/rs.3.rs-645086/v1

Abstract

A label-free electrochemical biosensor has been developed using Zinc Oxide nanoflowers (ZnONFs) for the detection of Uric acid. ZnONFs have been synthesized by hydrothermal process and characterized with several techniques such as Ultraviolet-Visible spectroscopy, Fourier Transform Infrared Spectroscopy (FT-IR) study, X-ray diffraction study, Raman spectroscopy, Scanning Electron Microscopy and High-Resolution Transmission Electron Microscopy (HR-TEM) and electrochemical analyser to confirms the formation of nanoflowers and fabrication of electrode and bioelectrodes for uric acid detection. Pure and uniform needle flowers and deposited onto Indium Tin Oxide (ITO) substrate through electrophoretic deposition technique. Further, electrochemical studies have been performed with immobilized enzymatic bioelectrode followed by various uric acid concentrations. It has been found that the fabricated biosensor shows high sensitivity (10.38 µA/ mg/mL /cm2) and a limit of detection of 0.13 mg/mL in the range of 0.005 to 1.0 mg/mL. This study demonstrates the potential use of ZnONFs for the construction of overly sensitive biosensors for Uric acid detection.

Introduction

Uric acid is an end product in the metabolic processes of purine nucleotides in the human body. Uric acid concentration can be examined by the spectrophotometric method, the method uses 4-aminoantipyrine and 2,4,6-tribromophenol as reactants, and uricase behaves as a biocatalyst. Permissible concentration of uric acid in the human serum is lies in the range of 0.15–0.45 mg/mL, for male is to be [237.9 ~ 356.9 µmol/L (4 to 6 mg/dL)] and for females is [178.4 ~ 279.4 µmol/L (3 to 5 mg/dL)] [1–2]. Presence of optimum amount of uric acid in the human serum is require maintaining the function of renal system but Further, increased in the concentration of uric acid beyond the allowed permissible limit can lead to severe chronic and acute diseases such as cardiovascular disease, hyperuricemia, hypouricemia, gout, arthritis and renal system problems, chronic kidney disease (CKD) [3]. Nanomaterials play an important role to improve the performance of biosensor devices due to high electrical, mechanical, optical, and catalytic properties Further improvement in the development of biosensor device is made using the remarkable nanomaterials such metal oxide and nanoparticle which lead to enhance the surface-to-volume ratio, biocompatibility, charge carrier mobility and mechanical flexibility. Biosensors are utilized for non-clinical as well as clinical laboratories using the specific bioreceptor bio-analyte system [4]. Various Uric acid biosensors are reported utilizing metal oxide nanoparticle and Uricase-Horseradish peroxidase (HRP) enzymes for fabrication of uric acid biosensors [5]. Chauhan et al. have developed a uric acid biosensor using the multiwalled carbon nanotubes as a transducer which is deposited onto Au electrode surface Uricase/AuNPs/MWCNTs/Au. Fabricated biosensor showed high sensitivity of 0.44 mA mM^{-1} in the linear range of 0.01–0.8 mM and limit of detection of 0.01 mg/mL. High stability and shelf-life of the bioelectrode surface demonstrates the effective immobilization of enzymes [6]. Muhsin ali et al. developed the Zinc Oxide quantum dots (ZnO QDs) based uric acid biosensors using uricase enzyme to fabricate the uric acid biosensor. This sensor possesses high sensitivity of 4.0 µA/mM cm^{-2} [7]. Shefali Jain et. al reported uric acid biosensor with sensitivity of 1.838 µA /(µM-cm2), LOD of 0.066 µM

with linear range of 0-700 µM by using butylamine capped spherical CZTS nanoparticles deposited onto ITO with uricase enzyme [8]. Castillo-Ortega et al. Constructed polyaniline-poly-n-butyl-methacrylate composite films immobilized with (urate oxidase) uricase enzyme for the detection of uric acid [9]. Zhang et al reported ZnS quantum dots based uric acid biosensors and the shelf life of constructed bio-electrode is around 20 days [10–11]. Kan et al. developed a polyaniline-uricase bio-electrode based biosensor via methods of the generation of hydrogen peroxide and its utilization by peroxidase that detect the decreasing level of dissolved oxygen concentration by the constructed biosensor. Liu et al. have constructed a bio-electrode in which a self-assembled monolayer containing a novel norbornylogous bridge by covalently attaching to flavin adenine dinucleotide (FAD), the redox active centre of several oxidase enzymes [12–13].

Sensitivity and selectivity of uric acid detection using uricase enzyme. uricase-Horseradish peroxidase enzyme immobilized onto ZnONFs/ITO electrode to fabricate uric acid biosensor. fabricated uric acid biosensor constructed with metal oxide nanomaterial to improve the sensitivity of bioelectrode with the help of enhanced surface to volume ratio of electrode [14]. Uricase enzymes used for detection of uric acid help to catalyse the oxidation reaction of uric acid and breakdown into Allantoin and H_2O_2 to produce electrons for sensitivity [15]. fabricated uric acid detection is mediator free [16]. This uric acid biosensor is based on electrochemical reactions occurring onto working electrodes. electrochemical signal produced from electron conductivity present in the buffer solution and process the electrochemical reactions. peak current variation depends on the concentration of uric acid [17–18]. in other testing practice of uric acid demands firstly collection of blood from patient and after collection unwillingly proceed it for segregation after following these procedure results take time at least 1–2 days but in biosensors for uric acid detection no need to follow this procedure basically this is a point of care (POC) technique. Biosensors not only detect only one analyte but are also able to detect different types of analytes such as, glucose, cholesterol, urea, uric acid etc [19]. In recent technologies there are several techniques developed to measure the concentration of uric acid in biological fluids. but biosensors are a unique and precise technique to detect uric acid concentration in biological fluids. This technique is cost effective, user friendly, accurate, precise, in POC grade, detection in wide range, real time detection, and gives results within a minute. For the fabrication of uric acid biosensors, there are several steps to be followed. In biosensors sensitivity is the main result to be measured that depends upon conductivity of bioelectrode. This bioelectrode has nanomaterial structures deposited on it. For this conductive nature many different metals, metal oxides, and carbon-based materials could be used in nanoform. metal oxide such as, TiO, MnO, MnO_2, SnO_2 etc [20–22]. Carbon based materials could be used such as CNT, carbon sheets, graphene, Graphene oxide, Reduced graphene oxides etc [23–24]. This work is focused on the fabrication of uric acid biosensors using the nanoflowers of ZnO. ZnO in nano form is highly remarkable materials because of specific properties such as, wide band gap (3.32 ev), semiconductor in nature, high isoelectric point (IEP) 9.5. ZnO exhibits high IEP value which directly gets attached with low IEP value of Uricase enzyme (4.5) results in strong physical bonding formation taking place between nanomaterial and enzyme that enhance the stability of the biosensor. Hydrothermal processes have been used to synthesize nanoflower and deposited onto indium-tin-oxide (ITO) surface using electrophoretic deposition

technique under the optimized applied voltage. Uricase-HRP enzyme was immobilized over the deposited ZnONFs electrode and electrochemical biosensing studies were performed with various concentrations of uric acid using the electrochemical analyzer. Electrochemical biosensor works in the range of 0.005 to 1.0 mg/mL concentration with sensitivity in the present work, ZnONFs based electrochemical biosensor is able to detect the uric acid concentration in the range of 0.005 to 1.0 mg/mL with sensitivity10.38 μA/ mg/mL /cm^2 and limit of detection (LOD) as of 0.13 mg/mL in buffer solution.

Experiments

Reagents and Materials

Uricase (Urate Oxidase, EC 1.7.3.3 from Bacillus fastidious, 9U/mg), Horseradish Peroxide (HRP), Uric acid (2,6,8-hydroxypurine, monosodium salt) from Sigma Chemical Co. St. Louis, Mo. Zinc Acetate ($C_4H_6O_4Zn$) Sodium hydroxide (NaOH), all utilized chemicals used from Sigma Aldrich without further purification. Potassium Ferrocyanide ($K_4[Fe(CN)_6]$), Potassium Ferricyanide ($K_3[Fe(CN)_6]$), Sodium-Dihydrogen phosphate (NaH_2PO_4), Sodium Mono-Hydrogen Phosphate (Na_2HPO_4), Aqueous solutions and buffers were prepared in Milli-Q water (18 MΩcm), Urea, Cholesterol, Ascorbic acid and Glucose.

Synthesis of Zinc Oxide Nanoflowers

Hydrothermal process is a promising method to synthesize nanostructures with controlled shape and size. Here, ZnONFs were synthesized using a low temperature method. In brief, a solution of 0.1M concentration of Zinc acetate ($C_4H_6O_4Zn$) and base Sodium hydroxide (NaOH) was prepared in 50 mL of deionized water. Thereafter, this solution was transferred into a Teflon seal tube and placed in a furnace at 80°C for 18h. After this the tube kept at room temperature to cool down and the synthesized material was washed with ethanol and Deionised water several times at 3000 rpm. After separating out precipitate, it was further incubated in a preheated incubator at 60° for 24 h to obtain Zinc Oxide powder.

Instruments

The ZnONFs were characterized using various techniques, such as UV-visible spectrophotometer (Lambda 950, PerkinElmer), Fourier Transform Infrared (FT-IR) spectroscopy (Spectrum BX, PerkinElmer) and X-Ray Diffractometer (Cu Kα radiation, Rigaku, JAPAN). Morphological investigations of ZnONFs have been studied using Scanning Electron Microscope (SEM) (SEM, LEO 440), High Resolution Transmission Electron Microscope (HR-TEM, Tecnai-G2F30 STWIN). Sensing measurements were recorded using (Autolab/Galvanostat/Potentiostat Eco Chemie, the Netherlands, model AUT 84275) in Phosphate-Buffer Saline (PBS, 50 mg/mL, 0.9% NaCl, pH 7.4) containing 5 mg/mL $[Fe(CN)_6]^{3-/4-}$ (redox species) utilized three electrode system, in this Ag/AgCl as Reference electrode and Platinum (Pt) as the Counter electrode at about 25 °C.

Synthesized ZnONFs deposition on ITO surface by Electrophoretic Deposition Technique

Before deposition of ZnONFs material over Indium Tin Oxide (ITO) substrate, first, ITO glass electrodes (Size:1 cm x 2 cm) were hydrolysed in solution containing 5:1:1v/v solution of water/H_2O_2/NH_3, respectively. Dipped ITO solution was placed in incubator at 70C for 30 minutes. Then, cleaned ITO were rinsed with distilled water and placed at room temperature. Further, two-electrode system having ITO as a working electrode and platinum as a reference electrode was used to deposit the synthesized ZnONFs onto ITO electrode under the applied voltage. Both dipped in ZnONFs powder solution dispersed in deionized water and deposited ZnONFs onto ITO electrode applying 8-11ev voltage. This ZnONFs/ITO electrode is further immobilized using Uricase-HRP enzyme to get Uricase-HRP/ZnONFs/ITO as a bio-electrode for uric acid sensing applications. [**Figure.1**] shows the schematic representation of electrophoretic deposition of ZnONFs onto ITO glass electrodes following fabrication of Uricase-HRP/ZnONFs/ITO bio-electrodes and its electrochemical response.

Fabrication of Uricase-HRP enzyme bio-electrode by physical adsorption

The Uricase-HRP/ZnONFs/ITO bio-electrode was constructed by a physical adsorption process. Firstly, the stock solution of Uricase-HRP enzyme (1mg/ml) has been prepared in a solution of tris-HCl buffer (1M) and HRP oxidase (0.5 mg/ml), Further (0.16 U/6µL) Uricase enzyme and 10µl of HRP drop casted onto ZnONFs/ITO electrodes. Thereafter, Uricase-HRP enzymes immobilized onto ZnONFs/ITO to construct Uricase-HRP/ZnONFs/ITO bio- electrodes into a high humid chamber for 3-4 h and then dried at room temperature. Finally, prepared Uricase-HRP/ZnONFs/ITO bio electrodes have been stored in the refrigerator at 0.4°C to be used further.

Results And Discussion

UV-Visible spectroscopy study

UV-Visible spectrophotometer has been utilized in the range of 250 to 850 nm using quartz cuvette for the optical study for synthesized ZnONFs. In [**Figure. 2**(a)] UV-Visible absorption peak observed at 370 nm for ZnONFs. This absorption peak indicates the presence of n-Π* antibonding due to the presence of lone pairs electrons of oxygen atom. This shift corresponds to the structure of ZnONFs. The energy band gap has been calculated and found to be 3.35eV indicates the formation of nanostructure [25].

Fourier-Transform Infrared spectroscopy study

The presence of functional groups in ZnONFs structure has been confirmed by FT-IR spectrophotometer. The characteristic peak of Zinc Oxide has been observed in [**Figure 2**(b)] which lies in the range of 400-550 cm^{-1} that confirms the bonding of Zn-O. The peaks appeared at 1410 cm^{-1} and 1575 cm^{-1} attributed to the C=O stretching vibrations and peak observed at 3050 cm^{-1} corresponds to the O-H stretching vibrations [26]. after the immobilization of uricase enzyme peaks appeared at around 3504 cm^{-1}, 2350 cm^{-1} corresponding to C=O stretching vibrations and O=H stretching respectively [27]. peaks appeared at 1558 cm^{-1} and 1649 cm^{-1} correspond to primary and secondary linkage of amide groups present in the

uricase enzyme. Peak absorbed at 511 cm^{-1} slightly shifted from 462 cm^{-1} confirms the presence of Uricase enzyme onto ZnONFs/ITO electrode. All additional peaks observed in **[figure 2 (b 1)]** confirm the immobilization of uricase enzyme and fabrication of Uricase-HRP/ZnONFs/ITO bio-electrode for sensing [28].

X Ray Diffraction pattern analysis

A typical X-ray diffractometer (RigakuMiniflex, JAPAN) source copper target 30 kV and 15 mA were used with a scan rate of 3˚/min. X-Ray diffraction patterns depicted in [**Figure 2** (c)] have 2θ (20 to 80) Fine and sharp peaks are observed at nine different positions in XRD crystallographic patterns corresponding to (100), (002), (101), (102), (110), (103), (200), (112), and (201) crystal faces. Observed peaks in this data well matched the certified XRD pattern of ZnO with (JCPDS Card No. 89-1397), this JCPDS card information revealed that synthesized ZnONFs is in Hexagonal Wurtzite form with crystalline in nature. The crystallite size of ZnONFs has been calculated to be 17nm. No peaks observed from impurities, which indicates that the product is pure [29].

Raman studies

Raman spectrum was recorded in the range from 100 cm^{-1} to 1000 cm^{-1} Raman shift. The Raman spectrum of ZnONFs is depicted in [**Figure 2** (d)], revealing. the formation of crystallographic ZnONFs. Raman scattering reveals that ZnONFs have hexagonal structure with C46v space group. Symmetry of ZnONFs structure shows that vibrations are Raman active in other possibilities for other factors such as lattice spacing, and the chemical environment determines the place of vibrational frequencies. Sharp and strong peak at 438 cm^{-1} of optical photon E_2h mode reveals that this structure has a good crystalline structure [30]. Peak at 99 cm^{-1} corresponds to E_2L low intensity mode that indicates this structure has some crystallite defects also [31].

Morphology Studies

Morphological studies of ZnONFs have been measured with SEM technique and results shown in [**Figure 4**]. The well-dispersed and uniform formation of surface indicated that it successfully deposited ZnONFs onto ITO electrodes. SEM images clearly demonstrated the presence of flower shaped nanoparticles [32].

Microscopic studies

Microscopic study of synthesized material is helpful to identify shape and size of nanomaterial. The High-Resolution Transmission Electron Microscope (HRTEM) images as shown in [**Figure 3**], demonstrates the information of interplanar distances by fringes image, structure, shape, and size of synthesized ZnONFs. These pictures indicate that irregular structure of ZnONFs consisting of simple needle flowers, have interplanar spacing (d) about 0.22nm for (100) planes. These results revealed that ZnO exhibits hexagonal structure. and size found to be 2.6 nm [33].

Electrochemical studies

The electrochemical studies of the fabricated electrode and bioelectrode has been performed using the cyclic voltammetry technique in a three-electrode system of Ag/AgCl as a reference electrode and platinum as a counter electrode in PBS, pH 7.4 (50 mg/mL, 0.9% NaCl) containing 5 mg/mL $[Fe(CN)_6]^{3-/4-}$ at about 25°C at scan rate (v) of 50 mV/s. The cyclic voltammograms of the ITO electrodes were measured before and after surface modification with ZnONFs and Uricase-HRP subsequently as shown in [**Figure. 5**(a)]. It has been found that bare ITO electrode shows (ipa) oxidation peak current & (ipc) reduction peak current values at 490 µA & -403.9 µA respectively. The increase in peak current values has been found after the deposition of ZnONFs onto ITO electrodes as 736µA, -522.8 µA respectively. This increment in the values is due to the potential of ZnONFs nanomaterials. After the immobilization of enzymes over the ZnONFs/ITO electrode, current value found to be decreased as 621 µA, -620.9 µA respectively. This happens due to the immobilization of heavy biomolecules of Uricase-HRP enzyme onto ZnONFs/ITO electrodes. In other cases, this reading can also reveal that the biomolecule behaves as an insulator for sensing. Uric acid biosensor with different concentrations (0.005-0.75 mg/mL). Uricase-HRP enzyme (0.16 U/6µl) has been used for the oxidation of uric acid ($C_5H_4N_4O_3$) into allantoin ($C_4H_6N_4O_3$) and H_2O_2.

Redox reaction occurs in PBS buffer solution onto Uricase-HRP/ZnONFs/ITO bio-electrodes.

Cyclic voltammetry response of Uricase-HRP/ZnONFs/ITO bio-electrodes obtained at scan rates from 10 to 100 mV/s and recorded curve is shown in [Fig.1(S)]. The CV curves revealed that I_{pa} and I_{pc} increased in both directions simultaneously by varying the scan rate values. Peak current ratio of Uricase-HRP/ZnONFs/ITO bio-electrode (I_a/I_c) found to be 1, which indicates the quasi-reversible behaviour of redox species. Inset image in **[Figure.1(S)]**, shows the redox current response of Uricase-HRP/ZnONFs/ITO bio-electrode plotted with respect to square root of scan rate. Anodic and cathodic peak current established with the help of given Equation 3 and 4 (Karimi-Maleh H.et al).

I_{ac}= -35.69µA+67.44 × 10-6 $(A^2mVs^{-1})^{1/2}$ [scan rate $(mVs^{-1})]^{1/2}$; R^2 = 0.995 (3)

I_{cc}= -16.13µA-54.60 × 10-6 $(A^2mVs^{-1})^{1/2}$ [scan rate $(mVs^{-1})]^{1/2}$; R^2 = 0.991 (4)

In the Randles-Sevcik equation, current peak intensity mainly depends upon two factors, first is the working electrode active surface area and second is the concentration of electro-active species which effectively contributes to the performance of biosensor. The value of diffusion coefficient (D) has been calculated using the Randles-Sevcik equation (Equation no. 5)

$Ip = 2.69\times105\ n^{3/2}\ AD^{1/2}V^{1/2}\ C$ (5)

In this equation, Ip stands for peak current (µA), n stands for number of electrons, C stands for conc. of redox species (5 mg/mL), D stands for diffusion coefficient, A stands for area of working electrodes, V stands for scan rate (50 mV/s). The calculated diffusion coefficient (D) values for ITO electrode,

ZnONFs/ITO electrode and for Uricase-HRP/ZnONFs/ITO electrode are found to be $5.5x10^{-2}cm^2\ s^{-1}$, $3.6x10^{-2}\ cm^2\ s^{-1}$, and $4.3x10^{-2}\ cm^2\ s^{-1}$ respectively. The high value of diffusion coefficient for ITO electrode than ZnONFs/ITO electrode indicates higher electron diffusion kinetics due to the presence of nanomaterial deposited onto ITO electrode in case of ZnONFs/ITO and this coating of nanomaterial improved the electron activity, surface to volume ratio, and kinetics of the reaction performed in the redox solution with the variation concentration of analyte. But after immobilization of Uricase-HRP enzyme over ZnONFs/ITO electrode, the diffusion coefficient value $4.3x10^{-2}cm^2\ s^{-1}$ found slightly lower as compared to ZnONFs/ITO electrode. It is because Uricase-HRP enzyme reduces the electron activity of material onto the bio-electrode surface because it behaves as a non-conducting layer and promotes the hindrance in the electron transfer process.

The surface concentration of ZnONFs/ITO electrode and Uricase-HRP/ZnONFs/ITO bio-electrode has been calculated using Brown Anson equation. Eq. no.6

$$Ip = n^2 F^2 I^* AV/4RT \quad (6)$$

Where, F is the Faraday constant (96,548 C mol^{-1}), n is the no. of electrons transferred in redox reaction, I* stands for surface concentration of ZnONFs/ITO electrode and Uricase-HRP/ZnONFs/ITO bio-electrodes, A is the surface area of the electrode (cm^2), V is the scan rate (50 mV/s), R is the gas constant (8.314 J/(mol/k)), T is the absolute temperature (298 k).

By using Brown-Anson model equation I* value of ITO electrode, ZnONFs/ITO, Uricase-HRP/ZnONFs/ITO electrode found to be $424.02x10^{-9}$ mol/cm2, $636.9x10^{-9}$ mol/cm^2, $537.3x10^{-9}$ mol/cm^2 respectively, The I* ZnONFs /ITO electrode has been found to be higher than ITO electrode reveals the improvement in the surface to volume ratio, provide easier path for electron transportation, and enhance current efficiency. But in case of Uricase-HRP/ZnONFs/ITO electrode, the I* value is slightly decreased due to presence of heavy bio molecules onto the surface matrix. These heavy molecules restrict the electron interaction and create hindrance in electron transportation [34].

Electrochemical biosensing study of uric acid

The biosensing response of the fabricated bioelectrodes have been recorded with various uric acid concentrations in the range of 0.005 to 0.75 mg/mL and curve response is depicted in **[Figure. 5(b)]**. It has been found that the current response is increased as by increasing the concentration of uric acid indicates the binding between enzyme and uric acid due to the increasing rate of H_2O_2 molecule, which increases the transfer number of electrons during the reaction process. The calibration curve has been plotted and depicted in **[Figure. 6]** shows that linear increment in the current value with increasing the concentration of uric acid in the range of (0.005-0.75 mg/mL) in PBS buffer solution indicates linear behaviour of the biosensor.

$$Ip = 753.38\ \mu A + 10.369\ \mu A/\ mg/mL\ /cm^2 \times \text{concentration (mg/mL)};\ R^2 = 0.98 \quad (7)$$

$$LOD = 3\sigma / m \quad (8)$$

Where σ is the standard deviation of blank solutions, m is the slope of the calibration curve.

The fabricated bioelectrode Uricase-HRP/ZnONFs/ITO bio-electrode shows sensitivity of 10.38 μA/mg/mL/cm^2 and theoretical LOD value (found to be 0.13 mg/mL) and experimental value of (0.005 mg/mL) which has been calculated by using Eq. no. 8. The value of sensitivity and LOD of Uricase-HRP/ZnONFs/ITO bio-electrode found in exceedingly high range because of some specific reasons such as, deposition of ZnONFs onto ITO electrodes that has improved the electron conductivity, electron affinity, electroactivity, surface to volume ratio of ZnONFs/ITO electrodes. In case of ferri-ferro buffer solution Fe+ reduced via heterogeneous electron transfer from fabricated bio-electrode. This fabricated Uricase-HRP/ZnONFs/ITO bio-electrode behaves as an electrical conductor and Pt electrode behaves as a potentiated (can control the energy of the electron initiated from bio-electrode). Due to the enhancement of electron conductivity from Uricase-HRP/ZnONFs/ITO bio-electrode, peak current found a slightly higher range in comparison to ITO electrodes. Enzyme immobilization process also plays a major role in detection of uric acid. Uricase-HRP enzyme is immobilized onto a material electrode surface followed by a drop casting process. Basically, Uricase-HRP enzymes help to oxidise uric acid into allantoin, CO_2, and H_2O_2. In the second process H_2O_2 releases electrons, these electrons initiate conductivity and give peak current after applying voltage. Electron conductivity increased with the concentration of uric acid in buffer solution.

Interference studies

Uric acid biosensor helps to regulate the concentration of uric acid in human blood serum, but in the human blood serum there are several other analytes present. Some of these analytes can interfere in this specific detection of uric acid. To analyse the interference study, in **[Figure.2(S)]** different analytes have been used to detect, such as Urea (2 mg/mL), Ascorbic acid (3.8 mg/mL), Glucose (5 mg/mL) and Cholesterol (3.8 mg/mL) were used.

$$\% \text{ interference} = [I_{FD} - I_{int}] \times 100 / I_{FD} \quad (9)$$

By using Eq. no. 9, the calculated value of interference with analyte found to be exceptionally low (less than 1) so this value is completely negligible. This proves that Uricase-HRP/ZnONFs/ITO bio-electrode is specific and selective for detection of uric acid in human blood serum. This proves that Uricase-HRP/ZnONFs/ITO biosensor can detect only uric acid in the human blood serum apart from the other analytes present in serum such as glucose, cholesterol etc.

Table 1 represented the performance of the fabricated uric acid biosensors in comparison to the earlier reported uric acid biosensors. Detection range and detection limit of Uricase-HRP/ZnONFs/ITO bio-electrode as reported in this paper is wider and higher than the other reported uric acid biosensors.

Table 1. Comparison of several fabricated biosensors and its activity with present work

Matrix	Sensitivity	Detection range	LOD	Reference
Uricase/AuNPs/MWCNTs/Au	0.44 mA mM^{-1}	0.01–0.8 mM	0.01 mM	[6]
UOx/Fc/Cu_2O/GCE	1.900 μA- mM^{-1} cm^{-2}	0.01–1 mM	0.0596 μM	[35]
Uricase/ZnONRs	0.1054 μA/mM	5 μM-3 mM	-	[11]
Naf/UOx/Fc/GCE	1.78 μA/μM	500nM-600μM	230 nM	[36]
Nafion/ZnOQDs/Uricase	4.0 μA/mM.cm^{-2}	1mM-10mM	22.97 μM	[7]
Butylamine capped spherical CZTS nanoparticles	1.838μA / μM/cm^2	0-700 μM	0.066 μM	[8]
CNF-RGO	0.14 μA/μM	100-700 μM	-	[37]
Graphene/Pt-GCE	0.41μA/μM	0.05-11.85 μM	-	[38]
Bacillus uricase/ PANI/MWCNT/ITO electrode	-	0.005–0.6 mM	0.005mM	[1]
Uricase-HRP/ZnONFs/ITO bio-electrode	10.38 μA /mg/mL/ cm^2	0.005-0.75 mg/mL	0.13 mg/mL	This work

Conclusion

In summary, we have fabricated a sensitive and selective uric acid biosensor ZnONFs. The ZnONFs helps to detect low concentration of uric acid because of its improved surface-to-volume ratio, enhanced electro catalytic properties and improved electrical redox behaviour. The Uricase-HRP/ZnONFs/ITO bio-electrode based biosensor helps to detect the uric acid concentration from 0.005 to 1.0 mM, exhibiting LOD

(0.13mM) in a redox probe. This biosensor shows high selective and specificity with high sensitivity of 10.38 μA/mM/cm^2.

Declarations

Acknowledgements

We are grateful to the Director, National Physical Laboratory, New Delhi, India, for providing research facilities. Priyanka Dutta is thankful to UGC for providing research fellowship.

Ethical Approval: This article does not contain any studies related to human participants or animal performed.

Consent to participate: Consent to participate was obtained from all individual participants included in this study.

Consent to publish: Consent to publish was obtained from all individual participants included in this work.

Conflict of interest: The authors declare that they have no conflict of interest.

Author's contribution: All authors as Priyanka Dutta, Vikash Sharma, Hema Bhardwaj, Ved Varun Agrawal, Rajesh, Gajjala Sumana have contributed equally to this work.

Funding: No special funding is received for this research work.

Competing Interest: The authors declare that they have no competing interest.

Availability of data and material: NA

References

1. Bhambi M, Sumana G, Malhotra BD, Pundir CS Biotechnol (2010). 38:178–185. https://doi.org/10.3109/1073119100371634.

2. Umar A, Rahman MM, Vaseem M, Hahn Y-B , Electrochem. commun (2009). b 11:118–1. https://doi.org/10.1016/j.elecom.2008.10.046

3. Arellano, F., & Sacristán, J. A. (1993). Ann. Pharmacother., 27(3), 337-343. https://doi.org/10.1177%2F106002809302700317

4. MacLachlan J, Wotherspoon ATL, Ansell RO, Brooks CJ W J. Steroid Biochem. Mol. Biol. (2000). 72:169–195. https://doi.org/10.1016/S0960-0760(00)00044-3

5. Bhargava AK, Lal H, Pundir CS J Biochem Biophys Methods (1999). 39:125–136 https://doi.org/10.1016/S0165-022X(99)00007-X

6. Chauhan N, Pundir CS Anal. Biochem. (2011). 413:97–103 https://doi.org/10.1016/j.ab.2011.02.007

7. Ali, M., Shah, I., Kim, S. W., Sajid, M., Lim, J. H., & Choi, K. H. (2018). Sensors and Actuators A: Physical, 283, 282-290. https://doi.org/10.1016/j.sna.2018.10.009

8. Jain S, Verma S, Singh SP, Sharma SN Biosens Bioelectron (2019). 127:135–141 https://doi.org/10.1016/j.bios.2018.12.008

9. Castillo-Ortega MM, Rodriguez DE, Encinas JC, et al Sens. Actuators B Chem. (2002). 85:19–25 https://doi.org/10.1016/S0925-4005(02)00045-X

10. Zhang Y, Wen G, Zhou Y, et al Biosens. Bioelectron (2007). https://doi.org/10.1016/j.bios.2006.08.038

11. Zhang F, Wang X, Ai S, et al Anal. Chim. Acta (2004). 519:155–160 https://doi.org/10.1016/j.aca.2004.05.070

12. Kan J, Pan X, Chen C Biosens. Bioelectron (2004). 19:1635–1640 https://doi.org/10.1016/j.bios.2003.12.032

13. Liu G, Gooding JJ Langmuir (2006). 22:7421–7430 https://doi.org/10.1021/la0607510

14. Alam, M. M., Asiri, A. M., Uddin, M. T., Islam, M. A., Awual, M. R., Rahman, M. M. (2019). New J Chem, 43(22), 8651-8659. 10.1039/C9NJ01287G

15. Rocchitta, G., Spanu, A., Babudieri, S., Latte, G., Madeddu, G., Galleri, G., Serra, P. A. Sensors, (2016). 16(6), 780. https://doi.org/10.3390/s16060780

16. Schöning, M. J., & Poghossian, A. (Eds.) Springer (2018). Vol. 1610.1007/5346-2017-2

17. Vijayakumar, A. R., Csöregi, E., Heller, A., & Gorton, L. "Anal. Chim. Acta" (1996), 327(3), 223-234 https://doi.org/10.1016/0003-2670(96)00093-1

18. Erden, P. E., & Kılıç, E. Talanta, (2013). 107, 312-323. https://doi.org/10.1016/j.talanta.2013.01.043

19. Bel'skaya, L. V., Sarf, E. A., & Kosenok, V. K. JOBCR (2020). 10(2), 59-65. https://doi.org/10.1016/j.jobcr.2020.02.004

20. George, J. M., Antony, A., & Mathew, B Microchim. Acta, (2018). 185(7), 1-26. https://doi.org/10.1007/s00604-018-2894-3

21. Chen, R., Wang, Y., Liu, Y., & Li, "RSC Adv", (2015). 5(103), 85065-85072. https://doi.org/10.1039/C5RA14328D

22. Zhu, H., Sigdel, A., Zhang, S., Su, D., Xi, Z., Li, Q., & Sun, S. Angew. Chem. Int. (2014). 53(46), 12508-12512. https://doi.org/10.1002/anie.201406281

23. Zhao, S., Wang, D. W., Amal, R., & Dai, L Adv Mat Res. (2019), 31(9), 1801526. https://doi.org/10.1002/adma.201801526

24. C. Wang, J. Li, X.Y. Luo, J.M. Hui, X. Liu, J. Tan, X. Zhao, Electroanal. Chem. (2016).780,147–2016.09.004 152.https://doi.org/10.1016/j.jelechem.

25. Imitan, S., Albonetti, S., Forni, L., Peri, F. and Lazzari, D. J. Colloid Interface Sci., (2009). 329, 73-80. https://doi.org/10.1016/j.jcis.2008.09.060

26. Rao NS, Rao MVB (2015). Am J Mater Sci 5:66–68

27. Sharma, A., Matharu, Z., Sumana, G., Solanki, P. R., Kim, C. G., & Malhotra, B. D. Thin Solid Films, (2010). 519(3), 1213-1218.https://doi.org/10.1016/j.tsf.2010.08.071

28. Matharu, Z., Pandey, P., Pandey, M. E., Gupta, V., & Malhotra, B. E. Electroynalysis (N.Y.N.Y.), (2009). .21(14), 1587-1596.https://doi.org/10.1002/elan.200904578

29. Bigdeli F, Morsali A, Retailleau P Polyhedron (2010). 29:801–806 https://doi.org/10.1016/j.poly.2009.10.027

30. Ramon C, Esther L, Jordi I, Luis A, Juan J, Buguo W and Michael J C, Phys. Rev. B, (2007). 75 165202.: 10.1103/PhysRevB.75.165202

31. Pal U, Garcia S J, Santiago P, Gang X, Ucer K B , Williams R T, Opt. Mater. (2006). 29 65.https://doi.org/10.1016/j.optmat.2006.03.015

32. Kashif M., Akhtar M.N., Nasir N., Yahya N Springer, Berlin Heidelberg (2010). vol 5. https://doi.org/10.1007/8611_2010_18

33. Karimi-Maleh H, Tahernejad-Javazmi F, Ensafi AA, et al Biosens. Bioelectron. (2014). 60:1–7. https://doi.org/10.1016/j.bios.2014.03.055

34. Nor NM, Razak KA, Lockman Z Electrochim.Acta (2017). 248:160–168. https://doi.org/10.1016/j.electacta.2017.07.097

35. Yan Q, Zhi N, Yang L, et al Sci Rep (2020). 1–10,10:. https://doi.org/10.1038/s41598-020-67394-8

36. Ghosh T, Sarkar P, Turner APF Bioelectrochemistry.(2015). 1–9,102: https://doi.org/10.1016/j.bioelechem.2014.11.001

37. Aryal, K. P., & Jeong, H. K Chem.Phys.Lett, (2020). 739, 136969. https://doi.org/10.1016/j.cplett.2019.136969

38. Sun, C. L., Lee, H. H., Yang, J. M, Wu, C. C. Biosens, (2011). 26(8), 3450-3455. https://doi.org/10.1016/j.bios.2011.01.023

39. Y. Zou, M. Zheng, W. Yang, F. Meng, K. Miyata, H. J. Kim, K. Kataoka, Z. Zhong Adv. Mater. (2017). 29, 1703285

Figures

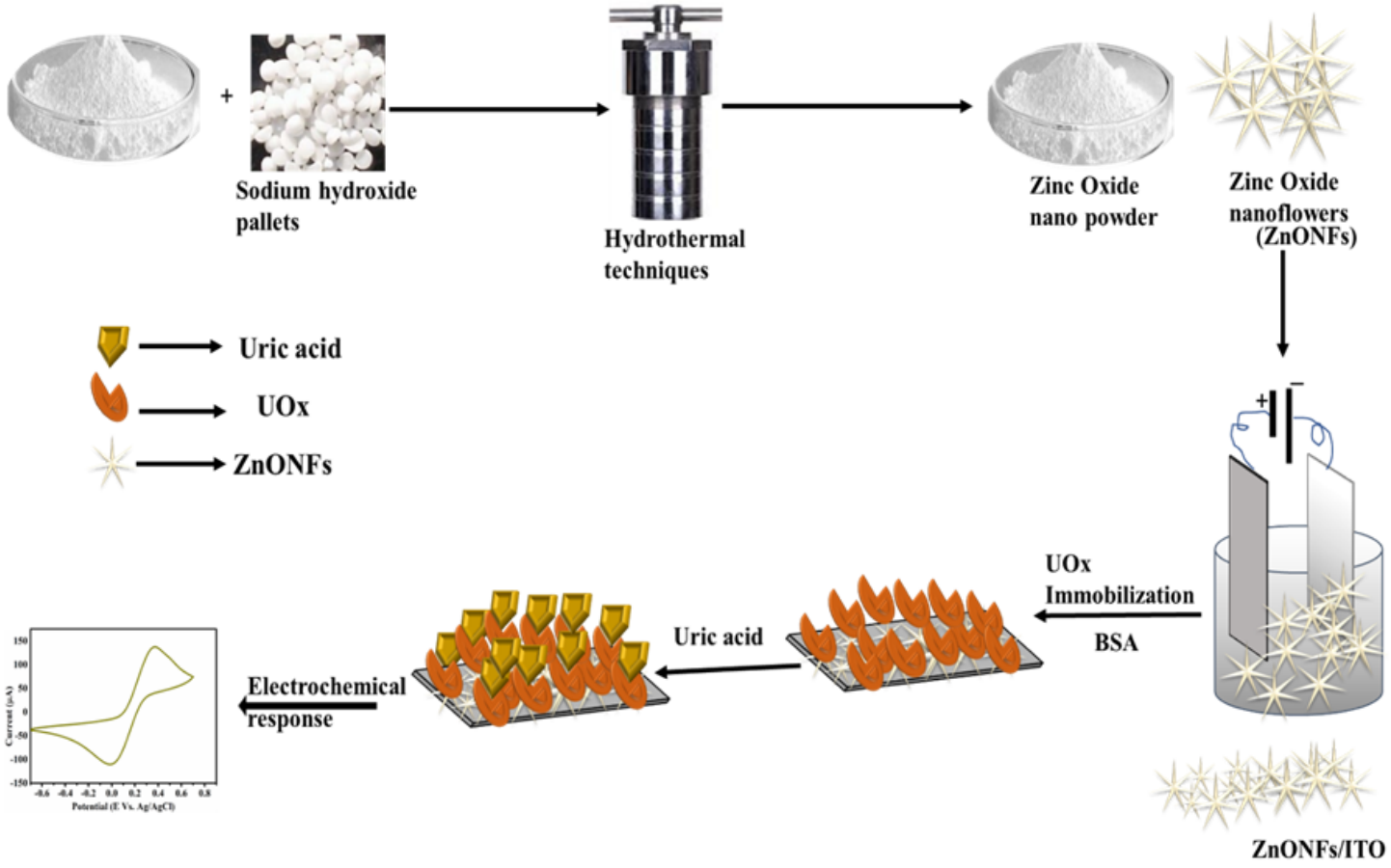

Figure 1

Schematic representation of fabrication of UOx/ZnONFs/ITO bio-electrode for uric acid detection using electrophoretic deposition ZnONFs/ITO electrode

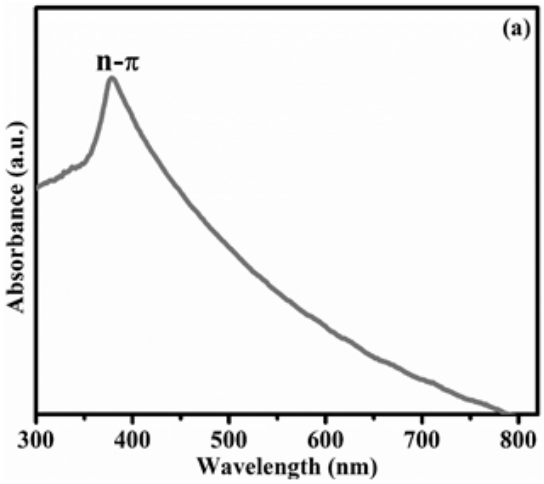

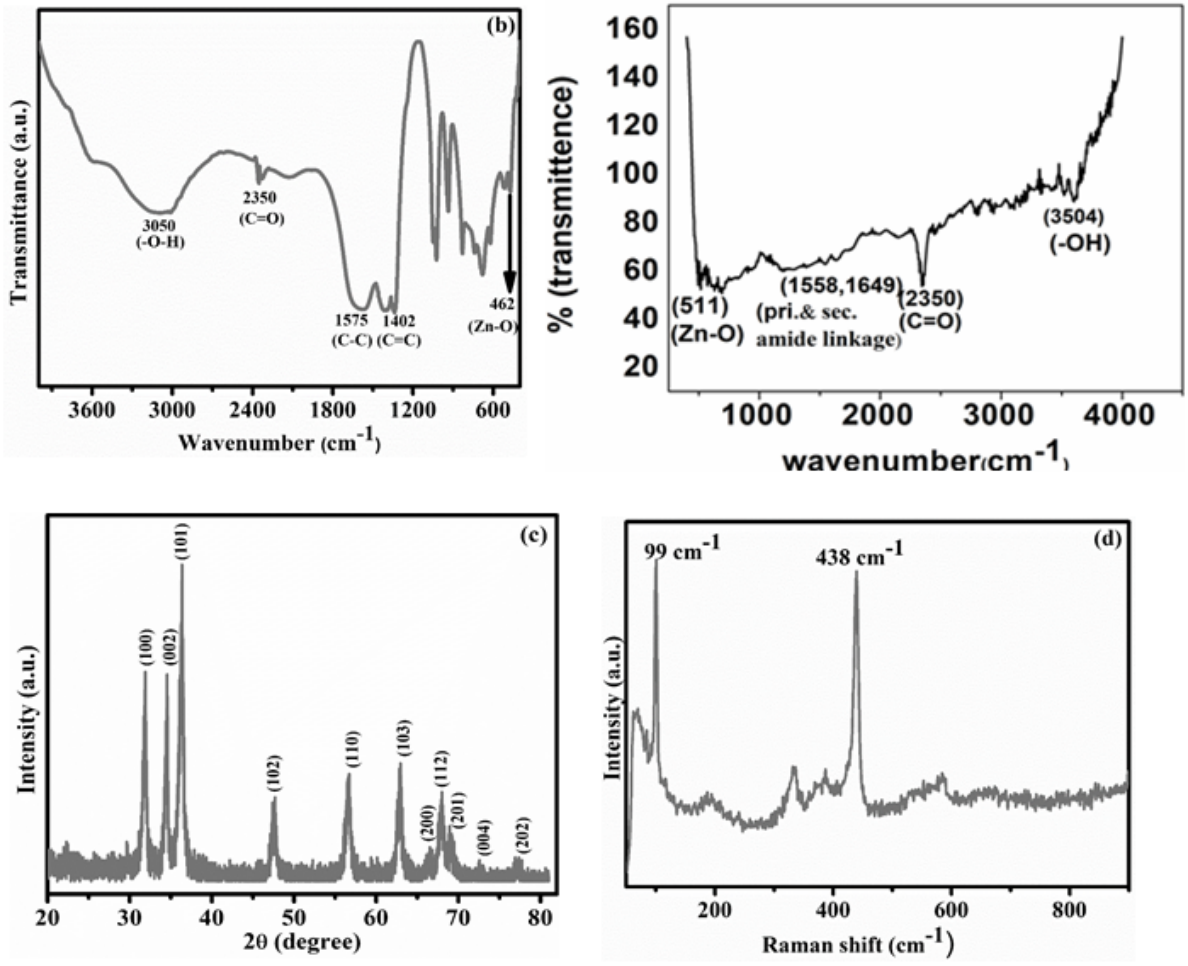

Figure 2

(a) UV-Visible spectra of ZnONFs, (b) FT-IR spectra of ZnONFs pellet, (c) X-ray diffraction pattern of ZnONFs powder, (d) Raman spectra of ZnONFs powder

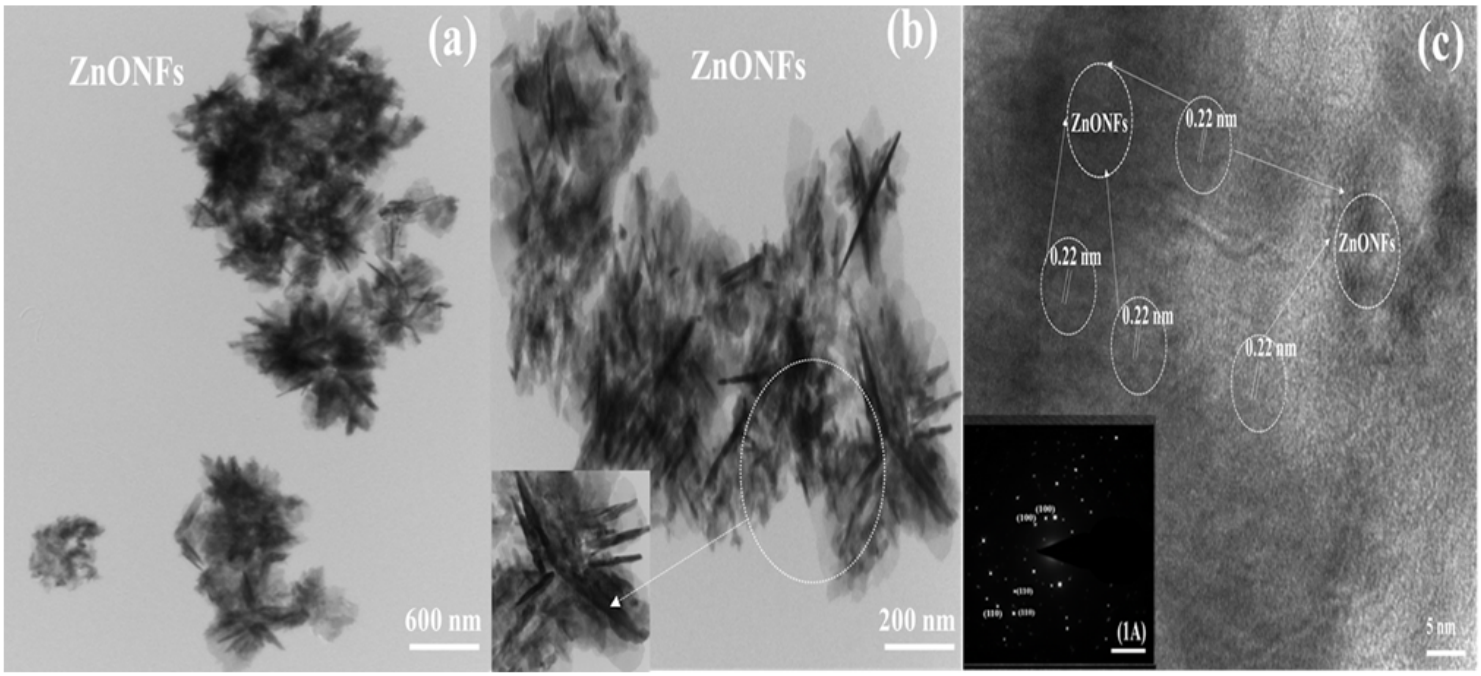

Figure 3

Transmission Electron Microscopy (TEM) images of ZnONFs

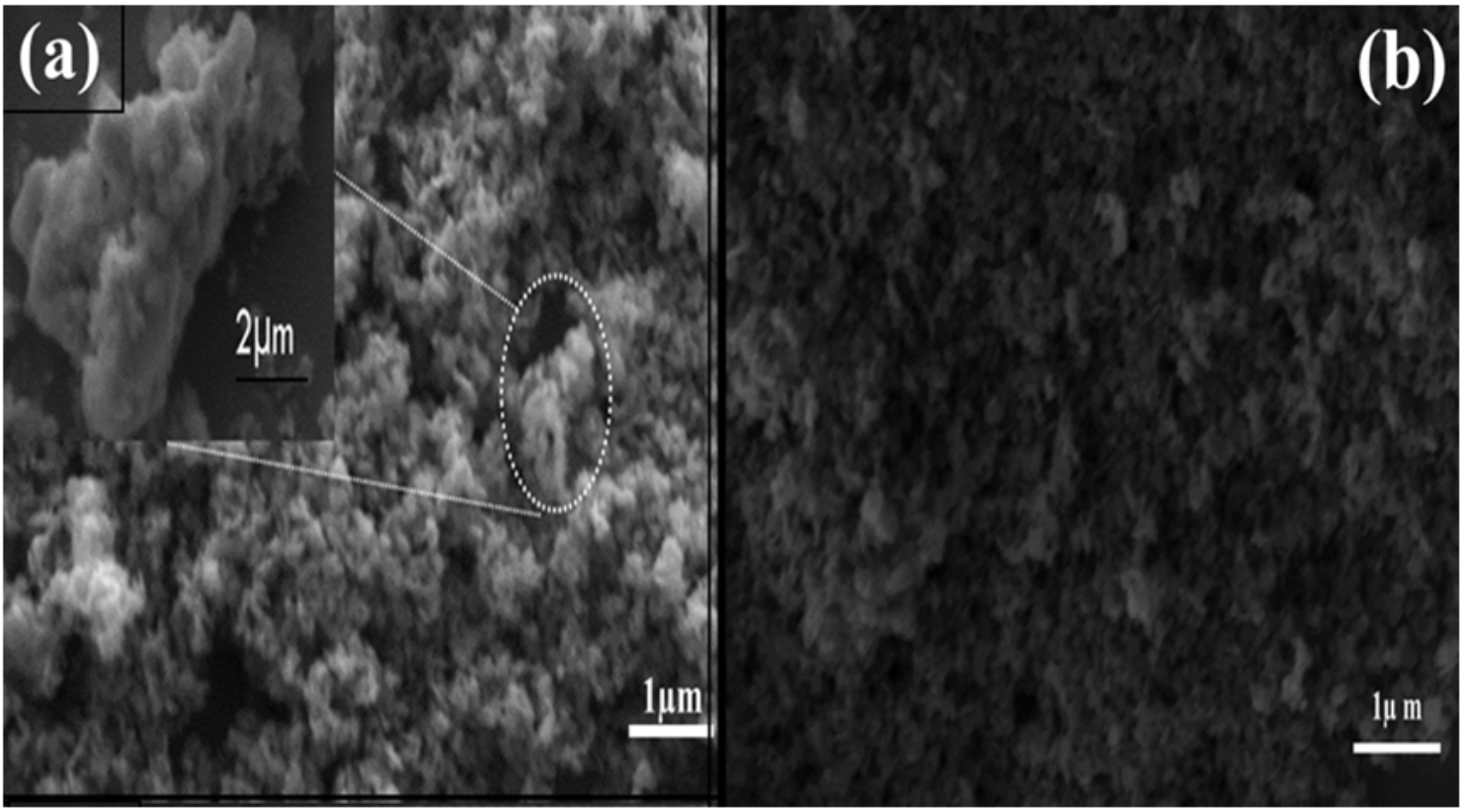

Figure 4

Scanning Electron Microscopic (SEM) images of ZnONFs/ITO electrode

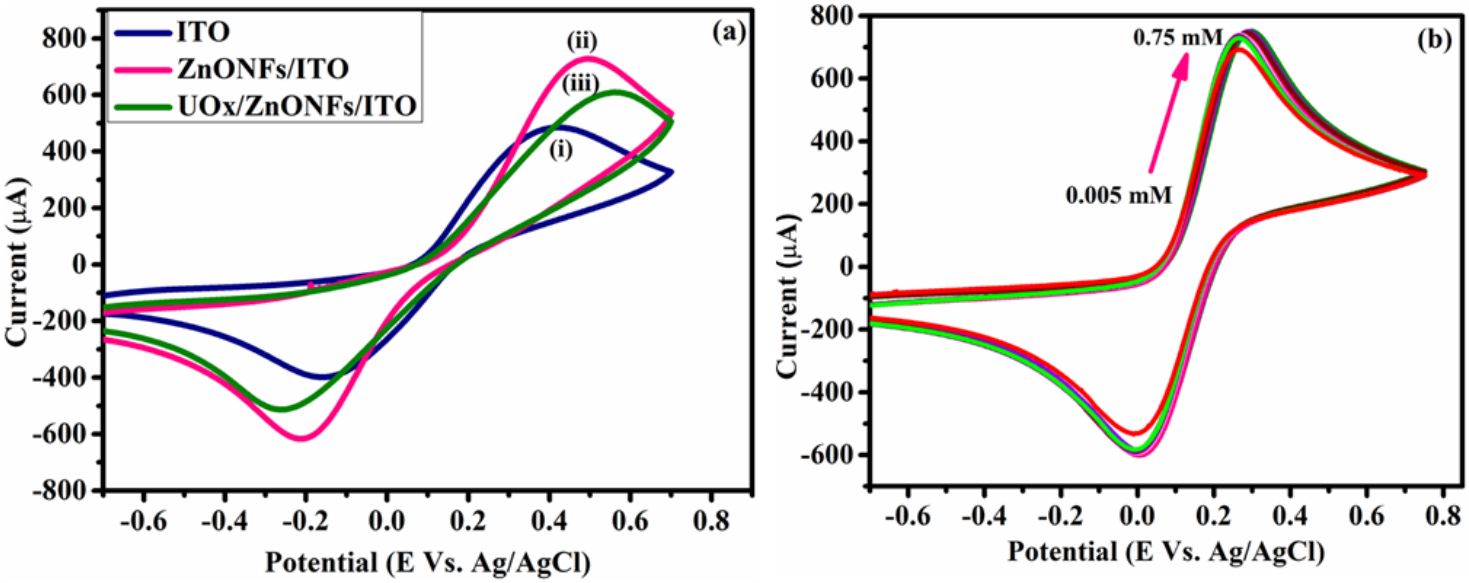

Figure 5

(a) Cyclic Voltammetry response of (i) ITO, (ii) ZnONFs/ITO electrode and (iii) Uricase-HRP/ZnONFs/ITO bio-electrodes conducted in 50 mM PBS (pH 7.4) containing 5 mM [Fe (CN)6]3-/4- redox species, (b) Cyclic voltammetry response of Uricase-HRP/ZnONFs/ITO bio-electrode with uric acid concentrations (0.005-0.75 mM) conducted in 50 mM PBS (pH 7.4) containing 5 mM [Fe (CN)6]3-/4- redox species

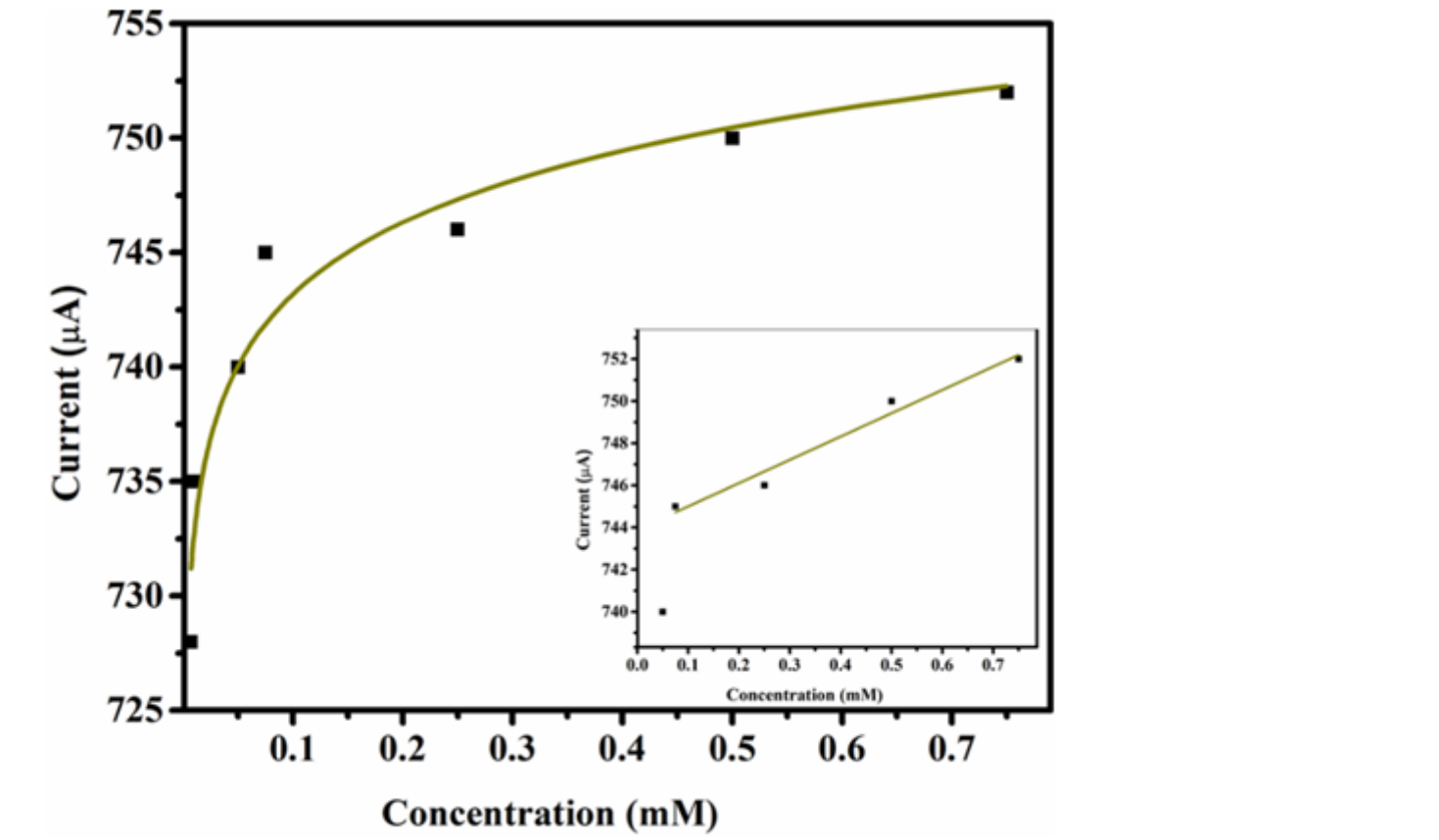

Figure 6

Calibration plot of current response with the function of analyte concentration ranging (0.005-0.75 mg/mL) conducted in 50 mg/mL PBS (pH 7.4) containing 5 mg/mL [Fe (CN)6]3-/4- redox species.

Supplementary Files

This is a list of supplementary files associated with this preprint. Click to download.

- supplymentryfileforAppliedBiochemistryandBiotechnology.doc